Applied Physics Letters

Self-driven formation and structure of single crystal platelets of Zn_3As_2

Cite as: Appl. Phys. Lett. **89**, 071901 (2006); https://doi.org/10.1063/1.2335682
Submitted: 24 April 2006 . Accepted: 26 June 2006 . Published Online: 15 August 2006

N. Kouklin, S. Sen, and M. Gajdardziska-Josifovska

Self-driven formation and structure of single crystal platelets of Zn_3As_2

N. Kouklin[a] and S. Sen
Departments of Electrical Engineering and Computer Science, University of Wisconsin-Milwaukee, P.O. Box 413, Milwaukee, Wisconsin 53201

M. Gajdardziska-Josifovska
Department of Physics and Laboratory for Surface Studies, University of Wisconsin-Milwaukee, Milwaukee, Wisconsin 53201

(Received 24 April 2006; accepted 26 June 2006; published online 14 August 2006)

In this work the authors introduce and provide details on the stoichiometrically controlled self-driven formation of freestanding single crystal platelets in Zn_3As_2 by a direct self-catalytic vapor-solid growth mechanism. The platelets feature dimensions of up to ~1 cm and mirrorlike microscopically flat top surfaces. A coherent formation of pyramids and wires has been further observed on some of the platelet top surfaces, the growth mechanism of which is discussed. This study might open pathways for facile engineering of high-performance semiconductor via a direct vapor-solid conversion of polycrystalline semiconductor powders into single crystal substrates on a large scale and with low cost. © *2006 American Institute of Physics*. [DOI: 10.1063/1.2335682]

Highly crystalline compound semiconductors lie at the heart of many modern device technologies. Their applications range from high-performance electronic devices, power conversion systems, solar cells, and photonic devices to biochemical sensors and microelectromechanical systems.[1–5] This success has been predominately based on the use of substrates featuring large size crystals, reduced defect densities, and increased purity. Stoichiometry controlled growth is additionally important in the case of compound semiconductors. A vast number of semiconductor growth methods are available and in use today with horizontal Bridgman (HB) and liquid encapsulated Czochralski (LEC) techniques being the best known for their application in the production of semiconductor wafers with reduced dislocation densities (HB) or increased diameters (LEC). Though these advantages have facilitated the realization of many microdevices that are in use today, certain technological limitations have prevented their widespread application for arbitrary semiconductor processing. Meanwhile, with the fast progression of basic semiconductor devices towards critical deep submicron and nanoscale dimensions[6,7] engineering of highly miniaturized lightweight devices, electromechanical systems, and "smart dust" sensors could be potentially accomplished on reduced (i.e., only centimeter or millimeter) size substrates. Therefore, the search for and development of alternative technologically viable routes that can afford for low-cost synthesis of freestanding semiconductor substrates suitable for electronic and optoelectronic nanodevice engineering is gaining importance today.

In this letter, we report on a possibility of employing chemical vapor deposition (CVD) processes for a two-dimensional stoichiometrically controlled synthesis of large scale (up to centimeter size) freestanding platelets as well as growth of small diameter wires in single crystal tetrahedrally coordinated zinc arsenide (Zn_3As_2) by a direct vapor-solid conversion route.

Zn_3As_2 is a member of II_3V_2 compounds that are currently attracting strong interest due to their close structural similarities with InP and InGaAs materials.[8] These materials, with high electronic mobility, low electron effective mass, and small direct band gaps (1.5–1.0 eV), have potential utilities in long wavelength optoelectronic devices, solar cells, and spintronics when doped with Mn. Moreover, the energy band gap can be easily tailored from 1 to 0 eV by alloying Zn_3As_2 with Cd,[9] making it highly promising for application in wavelength-tunable infrared detection and photovoltaics. In general, fabrication of highly crystalline and low strain Zn_3As_2 filmlike structures would be particularly required for many applications of this semiconductor in future photonics and electronics. Previously, a low strain synthesis has been realized by growing Zn_3As_2 on InP by molecular beam epitaxy (MBE) at low temperature ranges of ~300 °C; the achieved lattice mismatch was reportedly below 1%.[10] Requirement for using a lattice-matching substrate for MBE growth of Zn_3As_2 would, however, constitute a limitation with respect to process specifics, expected properties, and cost.

In this work Zn_3As_2 platelets were synthesized in a horizontally oriented CVD furnace operating in Argon atmosphere. Zn_3As_2 powders of 99% purity (grain size of 150 μm) were used as a source of Zn and As vapors when heated up to ~800 °C. To achieve uniform growth conditions across large length scales, powders were placed in specially designed alumina target holders with a cylindrical hole of 2–3 mm diameter that was found to provide more homogeneous target evaporation and maintain a better control on vapor stoichiometry with time. The temperature of the furnace was gradually increased from room temperature to ~800 °C in 60 min and maintained for another 60 min followed by a gradual cooling at the rate of ~5 °C min^{-1}. Before the growth, the CVD chamber was flushed several times by pumping it down to pressure of 10^{-3} Torr and subsequently filling the chamber with ultrahigh pure Argon gas that was also later used as a carrier gas for the growth. A very low flow rate of Ar was maintained at 0.1–0.3 SCCM (SCCM denotes cubic centimeter per minute at STP), so that

[a]Author to whom correspondence should be addressed; electronic mail: nkouklin@uwm.edu

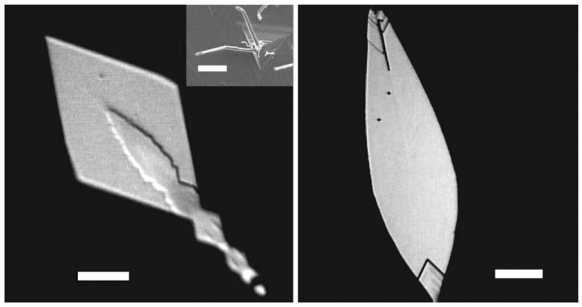

FIG. 1. Optical micrograph of as-grown Zn_3As_2 single crystal rhombus platelet (left), and other microstructures such as pyramids and wires as observed using SEM arising out of a platelet surface (inset) with the wires growing from the apex and side of the pyramids (bar in the inset is ~ 14 μm). On the right a leaflike platelet is shown (bars are ~ 1 mm).

the pressure inside the CVD chamber was close to atmospheric.

The morphology, crystal structure, and composition of the resulting platelets were characterized with reflection optical microscopy, scanning electron microscopy (SEM), transmission electron microscopy (TEM), selected area electron diffraction (SAED), energy dispersive x-ray Spectroscopy (EDS), and Raman spectroscopy.

Plain view optical microscope images of two typical forms of the platelet, i.e., rhombiclike and leaflike grown on the top surface of the fused alumina-silica substrate are shown in Fig. 1, left and right, respectively. Samples with a leaflike shape exhibit several times larger surface areas, while both types reveal microscopically flat, highly uniform, and mirrorlike surface on both sides. The length of the leaflike platelets (measured along the direction of growth) was found to occasionally approach $\sim 1-2$ cm, while their thickness was limited by $\sim 2-3$ μm according to SEM. Further examination of the leaf-shaped platelets further reveals the presence of an elbow-type structure at one of the tips. Despite the structural differences, both platelets show attachment to a substrate with a spear-shaped bladelike rod while their planes are oriented normally with respect to the top surface, therefore indicating that the platelet growth is likely to initiate at the rod surface. A more detailed examination of the platelets with SEM and TEM revealed that small diameter wires and micropyramids can occasionally grow from the crystal surface (inset in Fig. 1, left).

An EDS analysis has been next performed on the platelets. The EDS results, shown in Fig. 2, indicate only the presence of Zn and As constituents. Their peak intensity ratios show a close matching to that obtained on Zn_3As_2 target used to grow the samples, therefore confirming that the platelets are Zn_3As_2.

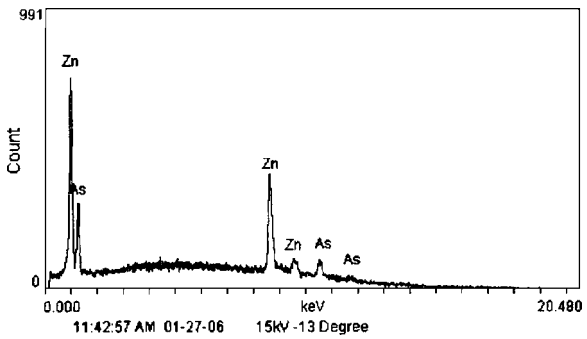

FIG. 2. EDS spectrum obtained on the Zn_3As_2 plates.

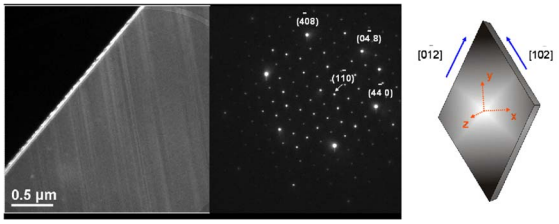

FIG. 3. Dark field TEM image of a platelet surface and edge (left) and representative SAED pattern obtained on the same platelet (middle). On the right: the identified main crystallographic orientations for the rhombic platelet is also shown with a separate coordinate system introduced to facilitate the visualization of the growth of the structures with x, y, and z directions corresponding to $[1\bar{2}2]$, $[1\bar{0}2]$, and [221] directions, respectively.

The crystal structure of Zn_3As_2 is well analyzed[10] and has an As sublattice with near similarity to zinc-blende III-V structures. The As sublattice has a slight tetragonal distortion (0.37%) of fcc cells along the c axis.[11] The Zn sublattice on the other hand is similar to that of the sublattice of fluorine in CaF_2 with 25% vacant Zn sites. These cation vacancies are ordered within the lattice. The As atom is tetrahedrally bonded to eight cavities of which two are vacant and six are occupied by Zn atoms. This leads to every Zn atom being tetrahedrally bonded to four As atoms. The unit cell is composed of 160 atoms and can be also viewed as stacked pseudocubic blocks with a small distortion in the lattice.

To identify the crystal parameters, a TEM analysis of the platelets was next performed. Owing to a good overall transparency of the as-grown platelets to electrons accelerated to energy of 300 keV, no sample thinning was required. The main result of the study is presented in Fig. 3, middle, which shows a typical SAED pattern obtained on the platelet from Fig. 3, left. The patterns obtained at various locations on the same and different platelets were completely identical and correspond to a [221] zone of the tetragonal lattice of Zn_3As_2. An experimentally measured value of a lattice constant in the $\langle 221 \rangle$ direction was ~ 2.08 Å, and the result is in a close agreement with that obtained through a direct calculation.

The formation of regular rhombic platelets is likely to be a result of simultaneous crystal growth proceeding via a self-catalytic route in positive and negative directions along two diagonals of the rhombic structure, depicted as the x and y axes in Fig. 3, right. However, the growth rates along xyz axes are different, giving rise to rhombic platelets of ~ 1 cm size and with thickness of a few microns only. A self-catalytic mechanism has been recently attributed to the growth of somewhat similar ZnO nano- and microsize belts, where zinc-terminated (0001) polar surfaces are considered more chemically active as compared to the oxygen-terminated (0001) ones.[12] The formation of pyramids on top of the platelets can be explained similarly with the only difference that the growth proceeds either in the positive or in the negative direction along x or y, making a triangle instead of a rhombus with included angle of $\sim 60°$, and with each consecutive layer serving as a substrate for the growth of the next layer. SEM analysis of pyramids indicates that their edges and sidewalls are not flat and have steps with their height occasionally approaching ~ 0.5 μm; these values, however, vary from sample to sample. The SAED pattern obtained on the pyramids is an exact replica of that of the platelet which strongly suggests that pyramids grow epitaxi-

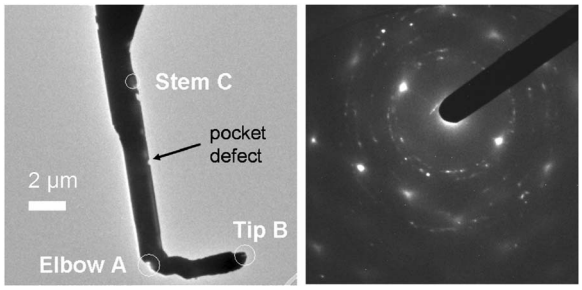

FIG. 4. TEM image of an elbowlike structure typically found at one of the ends (left); SAED pattern shows polycrystalline structure of tip (circular area B). SAED patterns obtained on multiple locations, including areas shown as A and C, confirm their structural similarity with the platelet.

ally on top of the platelet. Furthermore, the pyramids show identical orientation with respect to the platelet termination planes for all samples. Such crystallographically uniform self-ordering of pyramids is therefore attributed to be a property of Zn_3As_2 (221) planes.

In general, it is tempting to think that the rhombs should also exhibit a somewhat pyramidal structure. This, however, has not been confirmed experimentally. Instead, only a small tapering of the edges was identified with both TEM and SEM. This could likely point to the fact that the interplanar growth of Zn_3As_2 occurs at the initial stage, while the intraplanar growth dominates at the later stages, therefore yielding a centimeter-scale rhomblike planes with the thickness of only a few microns. It was also found that as-produced platelets can be precisely tailored with solid-state laser operating in a pulsed mode and in conjunction with an optical microscope, therefore offering a simple way to control the wafer geometry and its in-plane crystallographic orientation.

Finally, the presence of an elbowlike structure, Fig. 4, left, with a submicron diameter droplet at the very end of large size platelets was TEM analyzed. The resultant SAED image of the droplet is shown in Fig. 4, right, and confirms that it has polycrystalline structure, which does not match that of the platelet. Since As is relatively more volatile as compared to Zn, the target is likely to become depleted of As, resulting in the drop of partial pressures of As for prolonged times of growth. This in turn promotes nucleation of metallic Zn on the apex of platelets, shifting the growth mechanism towards a self-catalytic vapor-liquid-solid (VLS) growth mechanism, the latter being responsible for the elbow formation at the final stages of the growth. During the cool-down step the growth becomes strongly kinetically limited, and therefore shift in the growth mechanism can easily take place. An in-plane $\sim 90°$ turn in the growth direction could be confirmed for most of the elbows examined.

The diffraction patterns from multiple spots, including stem and edges of the elbowlike protrusion of the Zn_3As_2 platelets, revealed that the structures are single crystals and their crystallographic orientations exactly match that of the platelet, even though the temperature is expectedly lower for the last stage of the growth. A close-view examination of the upper part of elbow also reveals a zigzag chain architecture (Elbow A area on Fig. 4, left), that has been previously found for ZnO and attributed to a periodic switching between several equivalent growth directions.[13] While a further research effort will be critically required to clarify on the switching growth behavior in Zn_3As_2, the switching is generally attributed to a change in local growth parameters such as reduced temperature and vapor pressure, therefore promoting the formation of defect sites such as small pockets. The latter can easily trigger a change in the growth direction of the elbow as marked in Fig. 4, left, by a circle "Elbow A."

As outlined earlier, the performed SEM analysis also revealed that platelets can occasionally give rise to the growth of a pyramidlike structure on top of their surfaces. The results of comparative TEM and Raman studies (not shown) performed on both pyramids and platelets demonstrate their identical crystal orientation. Furthermore, some of the pyramid edges yield growth of the wires as well. The SEM investigation of the wires confirmed the presence of metal droplets at their tips—a typical attribute of catalyst-assisted VLS growth mechanism. This observation strongly implies that the plane edges can serve as nucleation sites of Zn particles as vapors become enriched with Zn. The particles can next act as catalyst in a secondary VLS growth of Zn_3As_2 wires. In general, this suggests that the platelets could potentially serve as a physical substrate for site-selective epitaxial production of Zn_3As_2 nanowires by CVD using Zn nanoparticles as a catalyst. The advantages of this approach will be minimized effects of unintentional doping and metal contamination, either of which could adversely redefine the electronic properties of nanostructured Zn_3As_2.

In this study, we reported on a self-catalytic growth of freestanding and microscopically flat platelets in Zn_3As_2 featuring dimensions up to ~ 1 cm. The results of EDS and electron diffraction studies performed on the samples confirm that the structure is a single crystal corresponding to the [221] zone of the tetragonal lattice of Zn_3As_2. In contrast to other fabrication techniques, this approach allows for a direct stoichiometrically controlled conversion of polycrystalline powders into single crystal freestanding small-size wafers by a vapor-solid growth mechanism. With the advent of nanotechnological paradigms for device engineering and continuous miniaturization of electronic devices offering both exponentially improved functionality and dramatically increased device packing density, the presented technique might open possibilities for mass-scale synthesis of quality lightweight millimeter and centimeter size substrates and single crystal nanowires in a variety of high-performance semiconductors with low cost.

[1] R. S. Wagner and W. C. Ellis, Appl. Phys. Lett. **4**, 89 (1964).
[2] H. Chik, J. Liang, S. Cloutier, N. Kouklin, and J. M. Xu, Appl. Phys. Lett. **84**, 3376 (2004).
[3] M. H. Huang, Y. Wu, H. Feick, N. Tran, E. Weber, and P. Yang, Adv. Mater. (Weinheim, Ger.) **13**, 113 (2001).
[4] H. Pan, S. Lim, C. Poh, H. Sun, X. Wu, Y. Feng, and J. Lin, Nanotechnology **16**, 417 (2005).
[5] G. Seryogin, I. Shalish, W. Moberlychan, and V. Narayanamurti, Nanotechnology **16**, 2342 (2005).
[6] H.-M. Kim, D. S. Kim, Y. S. Park, D. Y. Kim, T. W. Kang, and K. S. Chung, Adv. Mater. (Weinheim, Ger.) **14**, 991 (2002).
[7] Z. L. Wang, X. Y. Kong, Y. Ding, P. X. Gao, W. L. Hughes, R. S. Yang, and Y. Zhang, Adv. Funct. Mater. **14**, 943 (2004).
[8] D. M. Hwang, S. A. Schwarz, P. Mei, R. Bhat, T. Venkatesan, D. L. Nazar, and C. ML. Schwartz, Appl. Phys. Lett. **54**, 1160 (1989).
[9] M. J. Aubin, L. G. Caron, and J.-P. Jay-Gerin, Phys. Rev. B **15**, 3872 (1977).
[10] B. Chelluri, T. Y. Chang, A. Ourmazd, A. H. Dayem, J. L. Zyskind, and A. Srivastava, Appl. Phys. Lett. **49**, 1665 (1986).
[11] G. Pangilinan, R. Sooryakumar, B. Chelluri, and T. Y. Chang, Phys. Rev. Lett. **62**, 551 (1989).
[12] Z. L. Wang, X. Y. Kong, and J. M. Zuo, Phys. Rev. Lett. **91**, 185502 (2003).
[13] Pu Xian Gao and Zhong L. Wang, J. Appl. Phys. **97**, 044304 (2005).